energy&fuels

pubs.acs.org/EF

Article

Molecular Dynamics Insight into the Dissociation Kinetics of Hydrogen Hydrate Protected by Ice Shell

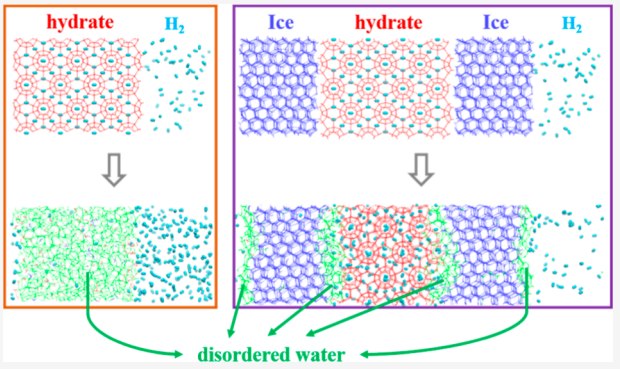
Siyuan Chen, Yang Du, Yanhong Wang,* Xin Lv, Shuanshi Fan, Xuemei Lang, and Gang Li

Cite This: *Energy Fuels* 2026, 40, 17616−17626

Read Online

ACCESS | Metrics & More | Article Recommendations | Supporting Information

ABSTRACT: Hydrogen hydrates are promising for hydrogen storage owing to high capacity and safety, yet the poor stability hinders its practical applications. This study used molecular dynamics simulations to systematically explore the stabilizing effect of an Ice Ih shell on hydrogen hydrates. At 260 K and 10 MPa, the quasi-liquid layer caused by the dissociation of hydrates retarded the diffusion of hydrogen from the hydrate to the gas phase but cannot prevent complete decomposition. In systems with an Ice Ih shell, structural transformation at the ice−hydrate interface dominates stability, strongly dependent on cage occupancy. Low-occupancy hydrates remain stable under superheating conditions, whereas high-occupancy ones fully dissociate as the ice shell converts to hydrate, thins, and collapses. This work clarifies the molecular stabilization mechanism of ice shell-protected hydrogen hydrates, offering a theoretical foundation for stable hydrogen storage and transportation via hydrate-based technologies.



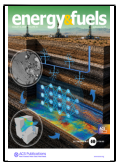
1. INTRODUCTION

Hydrogen energy, as a clean, efficient, and sustainable secondary energy source, serves as a key energy carrier for achieving the dual carbon goals. The development of suitable hydrogen storage and transportation technology is a critical step for the commercialization of the hydrogen energy industry chain.[1] Currently, the most common hydrogen storage methods include high-pressure gaseous storage, liquid hydrogen storage, and solid-state hydrogen storage.[2] Among these, solid-state clathrate hydrate-based hydrogen storage technology has attracted considerable attention as the characteristics of its high storage capacity, favorable safety, and reversible hydrogen storage−release.[3]

Clathrate hydrates, also known as gas hydrates, are non-stoichiometric crystalline compounds formed by host water molecules and guest molecules under high pressure and low temperature, which the water molecules are connected through hydrogen bonds to form cage-like frameworks.[4] Hydrogen molecules are encapsulated in the hydrate cages for the storage and transportation of hydrogen energy. Mao et al. synthesized sII hydrogen hydrates (consisting of 16 small cages (5^{12}) and 8 large cages ($5^{12}6^4$)) under conditions of 200−300 MPa and 240−249 K.[5] Their results indicated that the large and small cages were occupied by four and two hydrogen molecules, respectively (L4S2). Subsequently, it was reported that the storage capacity of hydrogen hydrates could reach up to 5.3 wt %,[6] demonstrating the great potential as a hydrogen storage medium. However, the poor stability of hydrogen hydrates poses a challenge for the transportation. As reported by Mao et al.,[6] the hydrogen hydrates stored up to 280 K exhibited excellent metastability only at 200 MPa, and the hydrates remained stable under atmospheric pressure only when cooled to 77 K. It was the first report on the preservation of hydrogen hydrate. Such stringent stability conditions severely limit its practical applications.

It has been confirmed that methane hydrates exhibited anomalous stability outside the thermodynamic stability region, retaining high stability at temperatures 50−75 K above their equilibrium temperature, which was referred to as the self-preservation effect.[7] The prevailing explanation for this effect was that the outer layer of hydrate decomposed below the freezing point and transformed into a surface ice shell, which suppressed further decomposition of the internal hydrate. Takeya et al. investigated the decomposition of methane hydrates at 253 K under atmospheric pressure and found that methane hydrates preserved for 24 h were tightly encapsulated by a thin ice layer. Even after one month, a high capacity of CH_4 remained inside the hydrate.[8] They further measured the decomposition rate of methane hydrates using energy-dispersive X-ray diffraction,[9] revealing that the decomposition process

Received: May 12, 2026
Revised: July 8, 2026
Accepted: July 23, 2026
Published: July 30, 2026



Downloaded from pubs.acs.org/enfuem/article-pdf/40/32/17616/6335445/acs.energyfuels.6c02515.pdf by SOUTH CHINA UNIV OF TECHNOLOGY user on 02 November 2026

ACS Publications

© 2026 American Chemical Society

https://doi.org/10.1021/acs.energyfuels.6c02515
Energy Fuels 2026, 40, 17616−17626

occurred in two stages: rapid initial decomposition of methane hydrates with the formation of an ice layer around the hydrates, followed by a reduced decomposition rate as the ice layer hindered CH_4 diffusion. Melnikov et al. first experimentally observed that when methane hydrate below the freezing point dissociated to supercooled water, which subsequently recrystallized on the hydrate to form a continuous protective ice layer, thereby enhancing the stability of methane hydrates.[10] Numerous studies have confirmed that ice shell can significantly delay hydrate decomposition. Based on these findings, researchers have proposed stabilizing gas hydrates by forming protective layers with the mechanism similar to the self-preservation effect, such as ice or other solid hydrate structures on the surface of hydrates.[11−13] Experimental studies have shown that external coating shell can construct a diffusion barrier on the hydrate surface, thereby impeding the escape of gas molecules and slowing the hydrate dissociation.[14] However, most existing studies focus on methane hydrates. Due to the high diffusivity and small molecular diameter of hydrogen molecules, whether the ice shell can hinder hydrogen diffusion within hydrate cages and further stabilize the hydrate structure remains to be explored.

In addition, the stability of hydrogen hydrates is closely related to the cage occupancy of the hydrogen molecules. Zhong et al. found that the stabilization energy of hydrogen hydrate generally decreased with increasing cage occupancy,[15] indicating that the hydrate cages with fewer hydrogen molecules were more stable. Niall et al. proposed that hydrogen diffusion was driven by enhanced nonequilibrium cage-to-cage hopping resulting from guest chemical potential equilibrium and concluded that double hydrogen molecules occupying the large cages and single molecules occupying the small cages were more stable (L2S1).[16,17] Gorman et al. investigated the molecular behavior of hydrogen hydrates using molecular dynamics (MD) simulations.[18] Their results showed that no hydrogen migration occurred with single hydrogen molecules in the small cages, while hydrogen migration appeared with the relaxation of hydrogen bonds when double hydrogen molecules were in the small cages, suggesting that single hydrogen occupation was more stable. Krishnan et al.[19] calculated the activation energy with different hydrogen cage occupancies using the Arrhenius equation and found that higher occupancy resulted in lower activation energy, which led to distortion of the hydrate structure; therefore, minimizing the occupancy of small cages was beneficial for structural stability. Burnham suggested that the cage occupancy of the large cages in hydrogen hydrates rarely exceeded two hydrogen molecules.[20] Although there is still debate regarding the exact number of hydrogen molecules occupying large and small cages in hydrates, it is widely accepted that the stability of hydrogen hydrates is strongly related to the hydrogen cage occupancy.

MD simulations provide an important tool for investigating the structural stability, migration behavior of guest molecules, and dissociation processes of gas hydrates. In this study, an MD simulation was employed to systematically investigate the stability of hydrogen hydrates. The dissociation behavior of the hydrogen hydrate systems with different cage occupancies was analyzed. Subsequently, the hydrogen hydrate systems with an ice Ih shell were constructed, and the influence of ice shell thickness on hydrate stability was further investigated. Parameters such as potential energy, number of water molecules, hydrogen migration fraction, and density distribution were used to elucidate the microscopic stability mechanism of hydrogen hydrates with an ice Ih shell. The study would provide guidance for the development of hydrate-based safe hydrogen storage technologies.

2. METHODOLOGY

2.1. Modeling

In this study, the TIP4P/ICE four-point water model[21] and three-point hydrogen model proposed by Alavi et al.[22] were used to describe the properties of water and hydrogen, respectively. The Lorentz−Berthelot combining rule was used to calculate the interaction between different molecules in the system.[23] The TIP4P/ICE model exhibits a certain deviation (25 K) in predicting the gas−liquid−solid three-phase point of gas hydrates;[24] however, the prediction of the freezing point and hydrogen hydrate stability aligns best with experimental data, which can better reflect the properties of hydrate.[25,26]

Hydrogen hydrate system was set as the control group. According to the work reported by Takeuchi et al.,[27] the hydrogen hydrate cell was constructed and subsequently expanded to a supercell with a size of 2.505 × 3.46 × 4.80 nm^3, containing 1048 water molecules. In this study, it was set up that four initial cage occupancies of L1S1, L2S1, L1S2, and L3S1 (L: $5^{12}6^4$ cages; S:5^{12} cages; the notation L_xS_y denotes x and y hydrogen molecules encapsulated in each large and small cage, respectively) corresponded to 160, 216, 264, and 272 hydrogen molecules. The gas phase was made up of 50 hydrogen molecules with a size of 2.505 × 3.46 × 2.40 nm^3. The total system size is 2.505 × 3.46 × 7.23 nm^3 (the initial configuration is shown in Supporting Information Figure S1).

Ice Ih was added to both sides of hydrogen hydrate in hydrogen hydrate with ice shell systems, consisting of ice shell−hydrogen hydrate−ice shell−gas phase (the initial structure is shown in Figure 1). As the size of the crystal cell of ice is

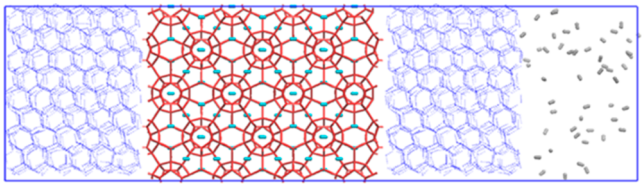


Figure 1. Initial configuration of hydrogen hydrate with the ice shell system: the hydrate structure is represented by red lines, the ice Ih structure is represented by blue, hydrogen in hydrate cages and gas phase are represented by cyan and silver spheres, respectively.

inconsistent with that of sII hydrogen hydrate crystal, so the size of ice shell was cut into 2.505 × 3.46 × 2.70 nm^3 and placed in system after the equilibrium simulation of 5 ns.[28] The ice shell on both sides of the system contained 756 water molecules and contacted the hydrate phase through the secondary prism plane. Previous studies have reported that lattice mismatch exists between ice and hydrate structures, and an interfacial transition layer was required to connect the two crystalline.[29] Therefore, no additional structural modification was performed at the ice−hydrate interface in this study. The configuration of the hydrogen hydrate and the gas phase was the same as described above. The overall size of the simulation system was 2.505 × 3.46 × 12.65 nm^3.

2.2. Simulation Details

All simulations were performed with GROMACS version 5.1.4.[30] A Nose−Hoover thermostat[31] (with a time constant

Downloaded from pubs.acs.org/enfuem/article-pdf/40/32/17616/6335445/acs.energyfuels.6c02515.pdf by SOUTH CHINA UNIV OF TECHNOLOGY user on 02 November 2026

https://doi.org/10.1021/acs.energyfuels.6c02515
Energy Fuels 2026, 40, 17616−17626

of 2 ps) and Parrinello−Rahman[32] (with a time constant of 4 ps) barostat were used to maintain the temperature and pressure, respectively. Periodic boundary conditions were applied in all of the directions. The particle mesh Ewald method[33] was used to calculate long-range electrostatic interactions. The cutoff radii for both van der Waals interactions and Coulomb interactions are set at 1.0 nm. All operating conditions adopt a single fully equilibrated initial supercell without repeated replicate trajectories. Identical force field parameters, boundary conditions, and simulation algorithms guarantee highly deterministic trajectory evolution for clathrate hydrate systems.

The simulation process is as follows: the initial configuration was first energy-minimized, followed by a 1 ns NVT equilibration. Subsequently, the NPT simulations were performed under 260 K and 10 MPa for 200 ns, which correspond to a metastable thermodynamic regime of hydrogen hydrates. At this temperature, the phase-equilibrium pressure of hydrogen hydrate is approximately 100 MPa,[34] indicating that the system is thermodynamically unstable. The primary purpose of this condition is not to reproduce long-term equilibrium or self-preservation behavior but to investigate the microscopic dissociation kinetics and structural evolution mechanisms. Under near-equilibrium or self-preservation conditions, the dissociation process would be extremely slow, making it difficult to observe statistically meaningful structural transitions within nanosecond scale simulations. Therefore, the chosen condition provides a suitable compromise between physical relevance and computational tractability, enabling a systematic comparison of the effects of cage occupancy and ice shell on hydrate stability. As for the hydrogen hydrate with an ice shell system, NVT simulations under 200 K were used for 10 ns for the adjustment of the interface between ice and hydrate phases. NPT simulations were conducted for 800 ns under 260 K and 10 MPa. The trajectories collected after the simulation were further processed via a time-averaged statistical analysis. More details about data analysis are available in the Supporting Information.

3. RESULTS AND DISCUSSION

3.1. Stability Analysis of Hydrogen Hydrates

Figure 2 shows the time evolution of the potential energy of hydrogen hydrate systems with different initial cage occupancies at 260 K and 10 MPa. It can be observed that a characteristic spike signifying hydrate dissociation in the potential energy was observed in all four systems. The curves eventually reached a stable plateau, indicating that the hydrogen hydrates had completely decomposed. This result suggested that the hydrate structures are unstable at 260 K and 10 MPa and fully dissociate regardless of cage occupancy. However, significant differences were observed in the hydrate dissociation behavior among the systems, in which the dissociation time increased with the cage occupancy: $t_{L1S1} < t_{L1S2} < t_{L2S1} < t_{L3S1}$. For the L1S1 system, the potential energy increased with a nearly constant slope, indicating that the hydrogen hydrate decomposed at an approximately constant rate. For the L2S1 and L3S1 systems, the dissociation process of hydrogen hydrate underwent three stages: rapid−slow−rapid dissociation; while the L1S2 system had only two stages, namely, slow dissociation followed by rapid dissociation.

To further analyze the effect of cage occupancy on the stability of hydrogen hydrates, Figure 3 presents the configurational snapshots of hydrogen hydrate systems with different initial cage occupancies. It can be observed that at 10 ns, hydrogen hydrates

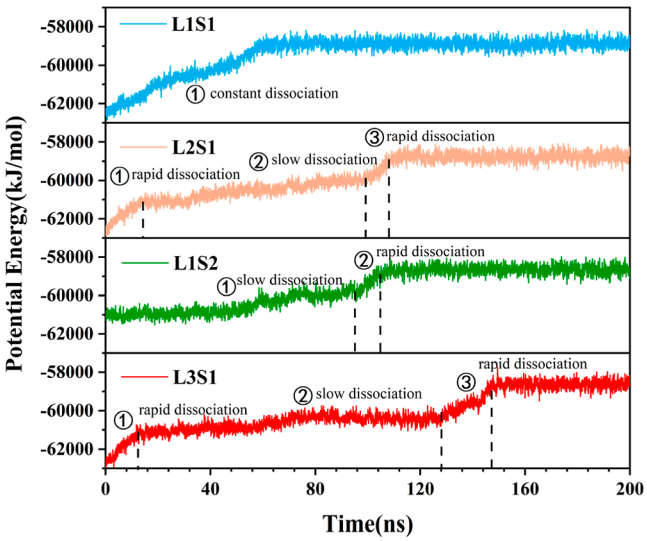


Figure 2. Potential energy evolution of hydrogen hydrate systems at 260 K and 10 MPa.

in four systems began to dissociate (rapid dissociation) at the hydrate−gas interface with hydrogen molecules migrated into the gas phase. As the L1S1 system with the lowest cage occupancy and minimum total hydrogen content, the residual hydrogen trapped within hydrate lattices was insufficient to sustain long-term structural stability, so the hydrate framework collapsed continuously at a steady and relatively rapid rate without a secondary dissociation stage afterward. The L1S2 system followed a two-stage dissociation pathway (slow dissociation followed by rapid dissociation). The hydrogen molecules in the 5^{12} small cages first migrated to the $5^{12}6^4$ large cages, forming a temporary slow dissociation period controlled by intercage hydrogen hopping, and then the hydrogen molecules diffuse outward (see Supporting Information Figure S2). Once most hydrogen molecules transferred out, the residual hydrate lattice lost stabilizing guest molecules and collapsed rapidly, which corresponded to the two-stage dissociation characteristics observed in the L1S2 system.

By contrast, the L2S1 and L3S1 systems with high large-cage hydrogen loading display three-stage dissociation kinetics (rapid−slow−rapid). At 40 ns, the L2S1 and L3S1 systems entered a slow dissociation stage because hydrate dissociation proceeded from the outer layer inward. A quasi-liquid film would form on the surface of hydrogen hydrates, and the dissociation interface shifted from the hydrate−gas interface to the hydrate−quasi-liquid film interface. Below the freezing point, the quasi-liquid film exhibited an "ice-like" structural ordering, which imposed significant mass transfer resistance to hydrogen molecules,[35] which trapped massive hydrogen inside the hydrate cages and formed an extended slow dissociation plateau. When the residual hydrogen concentration within the hydrate bulk dropped below the critical threshold required to maintain cage structural integrity, the entire hydrate lattice collapsed drastically and released a huge volume of hydrogen molecules, resulting in the second rapid dissociation stage.[36]

The L2S1 and L3S1 systems exhibited a similar characteristic of hydrate dissociation stages; however, there were significant differences in the dissociation time, mainly in the slow dissociation stage. Figure 4 shows the structural configurations of the L2S1 and L3S1 systems along with the time evolution of hydrate cages during the dissociation process. It can be observed

Downloaded from pubs.acs.org/enfuem/article-pdf/40/32/17616/6335445/acs.energyfuels.6c02515.pdf by SOUTH CHINA UNIV OF TECHNOLOGY user on 02 November 2026

https://doi.org/10.1021/acs.energyfuels.6c02515
Energy Fuels 2026, 40, 17616−17626

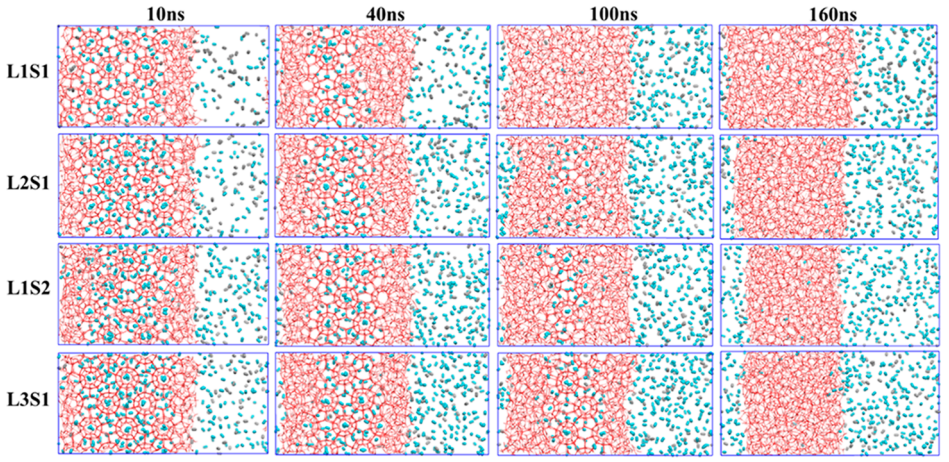


Figure 3. Snapshots of configuration of hydrogen hydrate systems at different times.

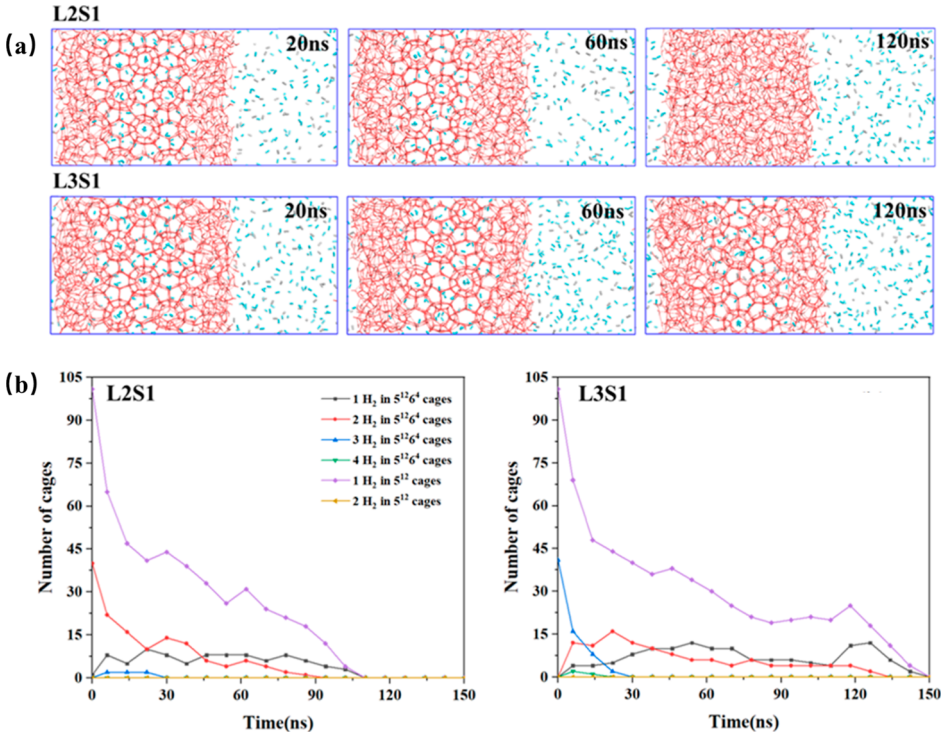


Figure 4. (a)Snapshots of hydrogen hydrate dissociation and (b) time evolution of cages with hydrogen molecules of L2S1 and L3S1 systems.

that at 120 ns, when the L2S1 system completely dissociated, the L3S1 system still retained some of the hydrate structure. This difference was mainly related to the migration behavior of the hydrogen molecules within the hydrate. During hydrate dissociation, hydrogen molecules in the $5^{12}6^4$ cages diffuse and migrate outward.[37] When hydrogen molecules in the outer hydrate layer diffuse into the gas phase, hydrogen molecules inside continuously move outward to replenish the outer layer. Therefore, the greater the number of hydrogen molecules occupying the $5^{12}6^4$ large cages, the longer the migration time required for hydrogen molecules to diffuse outward under the resistance of the quasi-liquid film, resulting in a longer slow dissociation stage. In the L2S1 and L3S1 systems, the quasi-liquid layer introduced an additional transfer resistance for hydrogen migration, thereby shifting the rate-limiting step from direct surface dissociation to diffusion through a disordered interfacial film, thereby slowing the dissociation rate. Consequently, the overall dissociation rate became significantly lower than that in the initial stage. However, it cannot prevent complete decomposition of the hydrate.

3.2. Stability Analysis of Hydrogen Hydrates with Ice Ih Shell

The stability of hydrogen hydrates with an ice Ih shell with different initial cage occupancies was investigated at 260 K and 10 MPa. Figure 5 shows the initial and final configurations of the hydrogen hydrate with ice Ih shell systems. Intermediate-time snapshots are not supplemented; continuous structural evolution during dissociation is supported by the time-dependent water molecules of hydrogen hydrate and ice in hydrogen hydrates (as shown in Figure 7). As shown in the figure, hydrogen hydrates did not completely dissociate, and some hydrate structures remained stable in the L1S1@Ice system after an 800 ns simulation. The behavior was quite different from that of the dissociation characteristics observed in

https://doi.org/10.1021/acs.energyfuels.6c02515
Energy Fuels 2026, 40, 17616−17626

Downloaded from pubs.acs.org/enfuem/article-pdf/40/32/17616/6335445/acs.energyfuels.6c02515.pdf by SOUTH CHINA UNIV OF TECHNOLOGY user on 02 November 2026

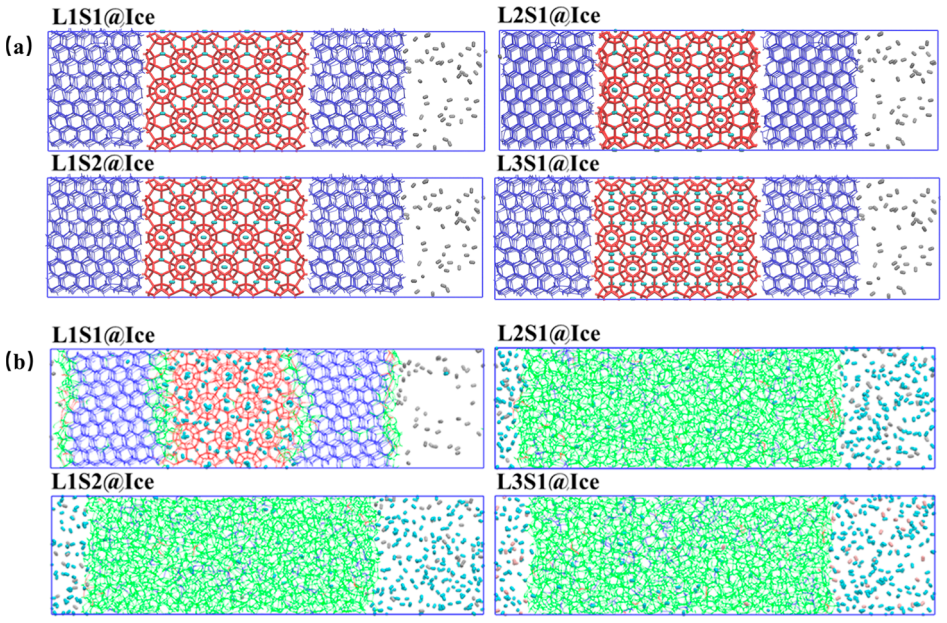


Figure 5. (a) Initial and (b) final configurations of the hydrogen hydrate with ice Ih shell systems.

the L1S1 system. In contrast, the hydrate and ice structures disappeared by the end of the simulation in the L2S1@Ice, L1S2@Ice, and L3S1@Ice systems.

The phase transition processes of hydrogen hydrates and ice were analyzed to further investigate the reason. Accordingly, the system was divided into six regions, denoted as A, B, C, D, E, and F (see Figure 6). The CHILL + recognition algorithm proposed

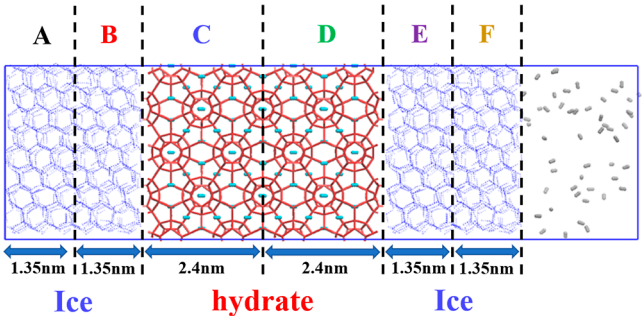


Figure 6. Region division of the number of water molecules in hydrogen hydrate with ice Ih shell systems.

by Nguyen et al.[38] was employed to identify water molecules in hydrogen hydrate and ice. Figure 7 shows the time evolution of the number of water molecules belonging to ice and hydrate phases in distinct regions of the hydrogen hydrate with ice Ih shell systems. Given the varying conditions of cage occupancy, each parameter's time axis was customized to match its own characteristic evolution window, with the time point defined as when the kinetic parameters cease to show obvious variations. For the L1S1@Ice system, the number of water molecules identified as ice in regions B and E increased from 300 to 350, while the number of water molecules identified as hydrogen hydrates remained zero in regions B and E throughout the simulation, which indicated that the water molecules at the ice−hydrate interface gradually became ordered into the ice structure. And the number of water molecules of ice phase in regions C and D increased significantly, accompanied by a decrease in the number of hydrate water molecules, indicating that part of the hydrate structure decomposed and transformed into ice in these regions. For the L2S1@Ice system, the number of water molecules in the ice phase in regions B and E decreased before 200 ns, while the number of water molecules of the hydrate phase increased markedly, suggesting that part of the ice shell decomposed into the hydrate phase. Subsequently, the number of water molecules of the ice phase dropped sharply after 200 ns, indicating that the original ice shell was destroyed. Approximately 15 ns after the destruction of the ice shell, the hydrogen hydrates began to dissociate. Such phenomenon was also observed in the L1S2@Ice and L3S1@Ice systems, with a difference in the dissociation times. In the L1S2@Ice system, the ice shell was disrupted at around 175 ns, and hydrate began to dissociate at approximately 270 ns. In the L3S1@Ice system, the number of water molecules of the ice phase decreased rapidly at 50 ns, while the number of water molecules of the hydrate phase began to decline at about 110 ns coated with ice Ih systems at 260 K and 10 MPa.

Table 1 compares the time required for complete dissociation of hydrogen hydrates with/without an ice shell. The L1S1 system exhibited the fastest dissociation kinetics among all of the systems. In contrast, the hydrogen hydrates in the L1S1@Ice system did not completely dissociate, which can be mainly attributed to the protective effect of the ice shell. Although the hydrogen hydrates in L2S1@Ice, L1S2@Ice, and L3S1@Ice systems completely dissociated within 800 ns, the dissociation times were significantly longer than those systems without an ice shell. This was primarily because the disordered water layer caused by the dissociation of the ice shell also hindered the diffusion of hydrogen molecules within the hydrate, thereby suppressing the dissociation of the hydrogen hydrates. Overall, the encapsulation of an ice shell can enhance the stability of hydrogen hydrates. However, during the stabilization process, structural transformations occurred between the ice and hydrogen hydrate. Once the ice shell was destroyed, it was difficult for hydrates to remain stable due to the vanished shielding effect of the ice shell.

Downloaded from pubs.acs.org/enfuem/article-pdf/40/32/17616/6633445/acs.energyfuels.6c02515.pdf by SOUTH CHINA UNIV OF TECHNOLOGY user on 02 November 2026

https://doi.org/10.1021/acs.energyfuels.6c02515
Energy Fuels 2026, 40, 17616−17626

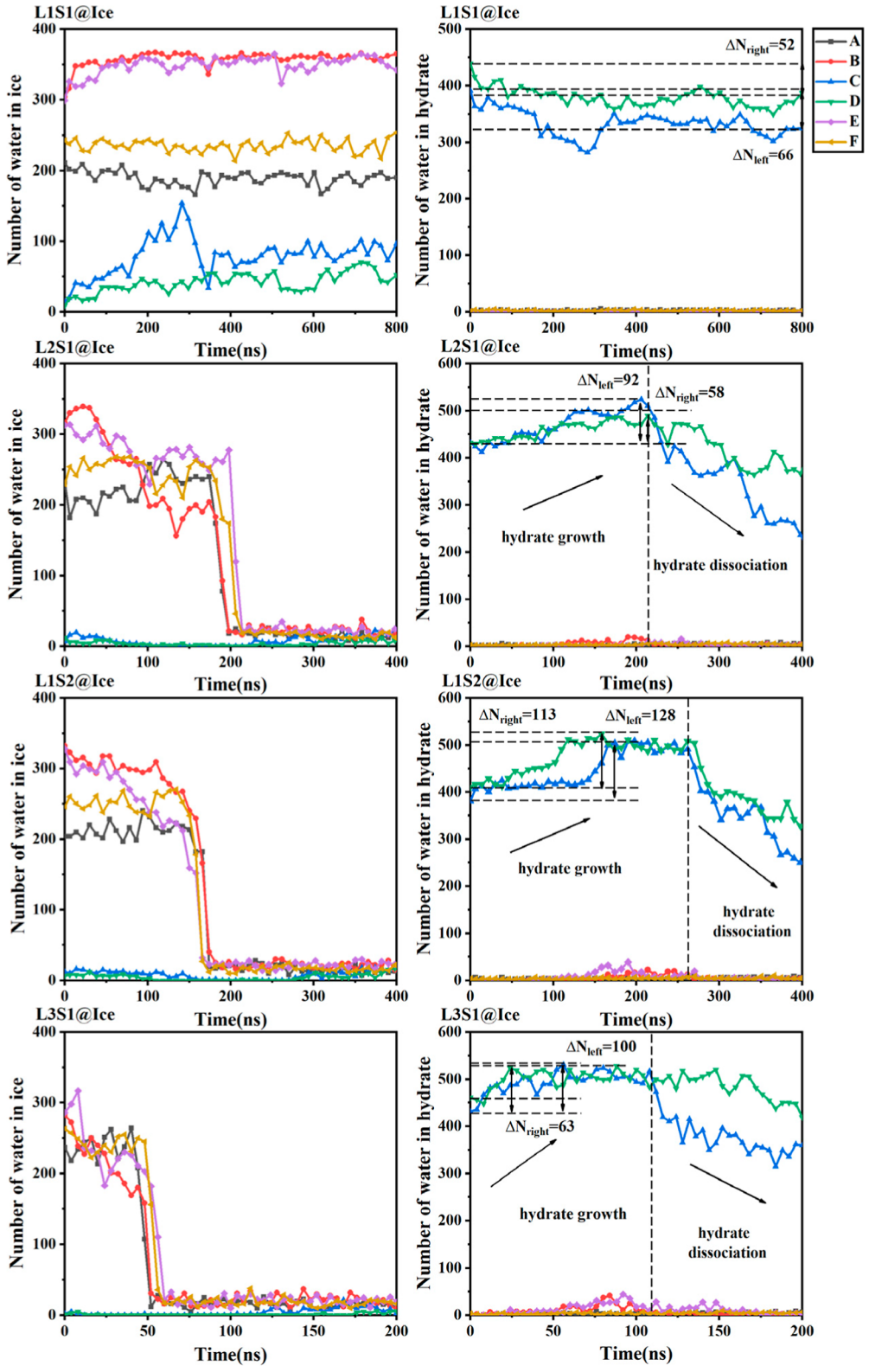


Figure 7. Number of water molecules of hydrogen hydrate and ice in hydrogen hydrate.

3.3. Effect of Ice Ih Thickness on the Stability of Hydrogen Hydrates

In the L1S1@Ice system, the ice shell gradually thickened, while in the L2S1@Ice, L1S2@Ice, and L3S1@Ice systems, the ice shell gradually thinned until eventually destroyed. This raised the question of whether hydrogen hydrates can be stably preserved if the initial ice shell thickness is increased. To address this issue, an L2S1@Extended-Ice system with an ice shell thickness of 3.66 nm was constructed. Figure 8 shows the configurational evolution and the number of water molecules in the ice and hydrate phases of the L2S1@Extended-Ice system at 260 K and 10 MPa. As shown in Figure 8a, the hydrogen

https://doi.org/10.1021/acs.energyfuels.6c02515
Energy Fuels 2026, 40, 17616−17626

Downloaded from pubs.acs.org/enfuem/article-pdf/40/32/17616/6335445/acs.energyfuels.6c02515.pdf by SOUTH CHINA UNIV OF TECHNOLOGY user on 02 November 2026

Table 1. Time for Complete Dissociation of Hydrogen Hydrate with/without Ice Shell Systems

initial cage occupancy	time for complete dissociation of hydrate(ns)	
	none	ice shell
L1S1	58	/
L2S1	115	618
L1S2	108	666
L3S1	148	800

hydrates in the L2S1@Extended-Ice system remained structurally stable with the ice shell throughout the simulation. In Figure 8b, the number of water molecules in the ice phase showed little change, whereas the number of water molecules in the hydrate phase increased from 850 to 1004. This indicated that part of the ice structure transformed into hydrate, and the ice structure remained stable until the end of the simulation. The comparative results clearly revealed that sufficient ice shell thickness was a prerequisite for long-term hydrate stabilization. When the ice shell was 2.70 nm, continuous ice-to-hydrate phase transformation at the ice−hydrate interface gradually consumed the outer ice layer, leading to shell thinning, structural collapsed, and complete hydrate dissociation within 800 ns. In contrast, the 3.66 nm thick ice shell provided abundant water molecules to sustain the ice−hydrate phase equilibrium; even partial ice was converted into hydrate at the interface, residual intact ice still maintained a complete diffusion barrier, so the hydrate phase can be stably preserved throughout the 800 ns simulation. It should be noted that only two ice thickness gradients were adopted in the current MD simulations, so a precise quantitative mathematical function linking ice shell thickness, cage occupancy, and hydrate stable preservation time cannot be derived yet. Nevertheless, the pairwise comparison between ice shell and extended-ice shell systems still delivered a clear qualitative rule: thicker initial ice shells significantly delay ice shell failure and extend hydrate survival time, especially for high-occupancy hydrate systems. In other words, the complete decomposition of hydrogen hydrates in the L2S1@Ice, L1S2@Ice, and L3S1@Ice systems can be mainly attributed to the insufficient thickness of the ice shell.

Figure 9 shows the variation in the number of hydrate cages in the L2S1@extended-ice system. Within 50 ns, the number of 5^{12} cages increased, indicating the growth of the hydrogen hydrates. During this period, the number of $5^{12}6^4$ cages occupied by two hydrogen molecules decreased (L2), while the number of $5^{12}6^4$ cages occupied by a single hydrogen molecule increased (L1). A possible explanation was that hydrogen molecules originally

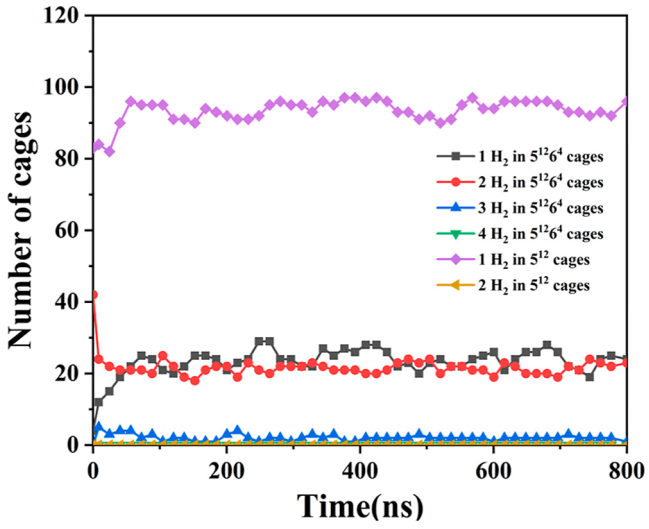


Figure 9. Number of cages in the L2S1@Extended-Ice shell system.

located in the $5^{12}6^4$ cages migrated into newly formed hydrate cages, resulting in a decrease in the occupancy of hydrogen molecules in the $5^{12}6^4$ cages. At equilibrium, the average occupancy of hydrogen molecules in the $5^{12}6^4$ cages was approximately 1.536, as calculated by the data after 50 ns. It could be seen that when the ice shell thickness increased to a certain extent, hydrogen hydrates grew within the confined space by the ice shell until a structural equilibrium between the ice and hydrogen hydrate phases was reached.

3.4. Mechanism Analysis of Hydrogen Hydrate Stabilization by Ice Ih Shell

Figure 10 presents the two-dimensional density distribution of hydrogen molecules in the hydrogen hydrate with ice Ih shell systems. In the L1S1@Ice system, hydrogen molecules were mainly concentrated in the hydrate phase at 800 ns, only few hydrogen molecules in the ice regions, and almost no hydrogen molecules in the gas phase. This indicated that during the simulation process, hydrogen molecules did not migrate from the hydrate phase into the gas phase, suggesting that the ice shell provided an effective barrier to hydrogen diffusion. In addition, in the L2S1@Ice and L1S2@Ice systems, the ice shell was destroyed at around 170−180 ns, and hydrogen molecules in the hydrate phase already migrated into the gas phase by 200 ns. In the L3S1@Ice system, the ice shell was disrupted at approximately 50 ns, and hydrogen molecules originating from the hydrate phase can be detected in the gas phase at 100, 150, and 200 ns. A common feature of these three systems was that

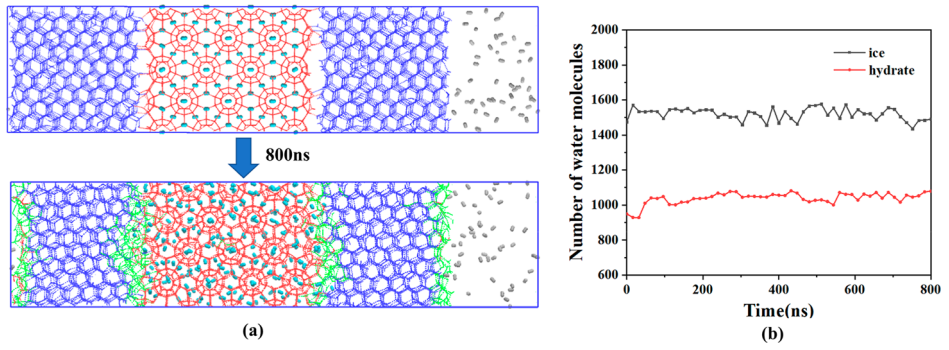


Figure 8. (a) The initial and final configurations of L2S1@ Extended-Ice shell system; (b) the number of water molecules in hydrate and ice.

https://doi.org/10.1021/acs.energyfuels.6c02515
Energy Fuels 2026, 40, 17616−17626

Downloaded from pubs.acs.org/enfuem/article-pdf/40/32/17616/6335445/acs.energyfuels.6c02515.pdf by SOUTH CHINA UNIV OF TECHNOLOGY user on 02 November 2026

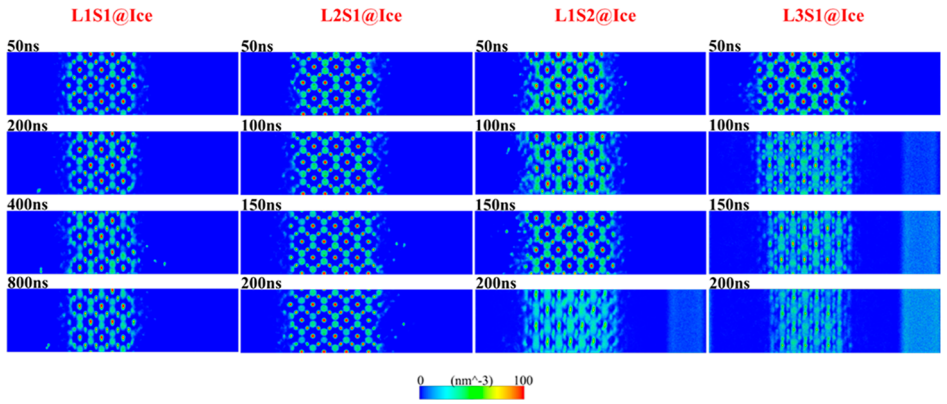


Figure 10. Density distribution of hydrogen molecules in hydrogen hydrate with ice Ih shell systems.

the ice shell completely dissociated during the simulation, indicating that once the ice shell was destroyed, its ability to hinder hydrogen diffusion was significantly weakened. Consequently, hydrogen molecules were distributed in both the hydrate phase and the gas phase. These observations further confirm that the ice shell plays an important role in blocking hydrogen migration.

Figure 11 shows the diffusion coefficients of hydrogen molecules within the hydrate phase. At 100 ns, the diffusion

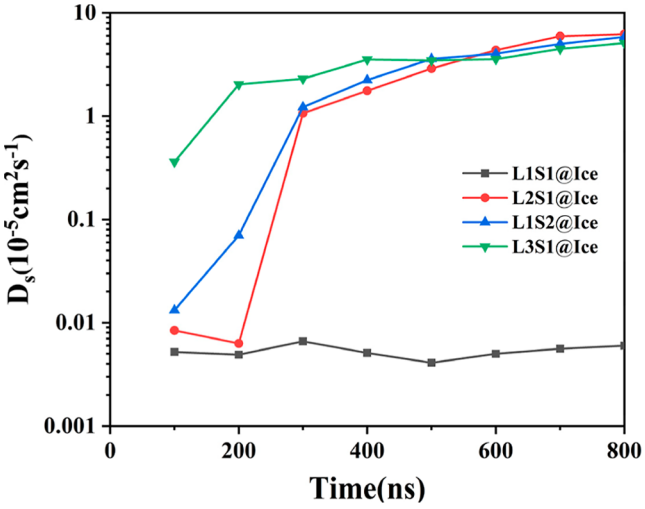


Figure 11. Diffusion coefficient of hydrogen molecules in hydrogen hydrate with ice Ih shell systems.

coefficient of hydrogen molecules in the hydrate phase of the L3S1@Ice system was significantly higher than that of the other three systems. This was because the ice shell in the L3S1@Ice system was destroyed at around 50 ns, while the ice shell in the other three systems remained stable. The mass transfer resistance provided by the ice shell restricted the motion of hydrogen molecules. In the L1S1@Ice system, the ice shell remained intact throughout the simulation, resulting in the lowest diffusion coefficient, which was approximately 3 orders of magnitude lower than that in the other systems. The results indicated that the motion of hydrogen molecules was strongly confined by the ice shell. In contrast, once the ice shell disappeared, the disordered quasi-liquid film provided much weaker resistance to hydrogen diffusion, allowing hydrogen molecules to pass through the disordered water layer and enter the gas phase more freely. For the L2S1@Ice system, the diffusion coefficient of hydrogen increased from 0.0063×10^{-5}·cm^2·s^{-1} (at 200 ns) to 1.0651×10^{-5}·cm^2·s^{-1} (at 300 ns). And the diffusion coefficient further increased to 6.2196×10^{-5}·cm^2·s^{-1} by 800 ns. It could be found that when the hydrates was stably encapsulated by the ice shell, the hydrogen molecules could be confined in the hydrate region for the stable preservation of hydrogen hydrates. However, once the ice shell was destroyed, the high hydrogen diffusion coefficients made it difficult to retain hydrogen molecules within the hydrate phase.

The fraction of hydrogen migration was used to evaluate the potential of hydrogen molecules in $5^{12}6^4$ cages or 5^{12} cages. As shown in Figure 12a, the final fraction of hydrogen migration in $5^{12}6^4$ cages in the L1S1@Ice system was the lowest, indicating the relatively low kinetic energy. As the number of hydrogen molecules occupying the $5^{12}6^4$ cages increased (L1 to L3), the fraction of hydrogen migration in $5^{12}6^4$ cages also increased, which was caused by more frequent guest−guest molecular collisions, making it easier for hydrogen molecules to migrate to neighboring cages.[19] It was also noteworthy that the fraction of hydrogen migration in $5^{12}6^4$ cages in the L1S2@Ice system was higher than that in the L1S1@Ice system. As shown in Figure 12b, the fraction of hydrogen migration in 5^{12} cages of the L1S2@Ice system was close to 50%, significantly higher than that in the other three systems, which indicated that the 5^{12} cages cannot stably accommodate two hydrogen molecules, and hydrogen molecules would tend to migrate to the $5^{12}6^4$ cages. Consequently, the increasing number of hydrogen molecules in the $5^{12}6^4$ cages would thereby increase the fraction of hydrogen migration in $5^{12}6^4$ cages. Overall, the increase in the hydrogen occupancy of either the $5^{12}6^4$ cages or the 5^{12} cages would lead to a high kinetic energy of hydrogen molecules. As a result, more hydrogen molecules overcame the cage confinement and migrated between hydrate cages.

For the systems with high cage occupancy (L2S1, L1S2, L3S1), abundant hydrogen molecules were confined inside the hydrate cages with strong intercage hopping tendency. Driven by chemical potential difference, hydrogen molecules continuously migrated from the hydrate matrix into the ice Ih shell. Hydrogen molecules trapped within ice lattice defects broke the ordered hydrogen-bond network of hexagonal ice, and the ice−water interface undergoes phase transformation. Belosudov et al.[39] reported that the thermal expansion coefficient of hydrogen hydrates was larger than that of ice. Consequently, ice Ih can exert an additional pressure (P_d) on hydrogen hydrates to stabilize the hydrate structure. From the thermodynamic perspective, as the additional pressure increased, hydrogen

https://doi.org/10.1021/acs.energyfuels.6c02515
Energy Fuels 2026, 40, 17616−17626

Downloaded from pubs.acs.org/enfuem/article-pdf/40/32/17616/6633545/acs.energyfuels.6c02515.pdf by SOUTH CHINA UNIV OF TECHNOLOGY user on 02 November 2026

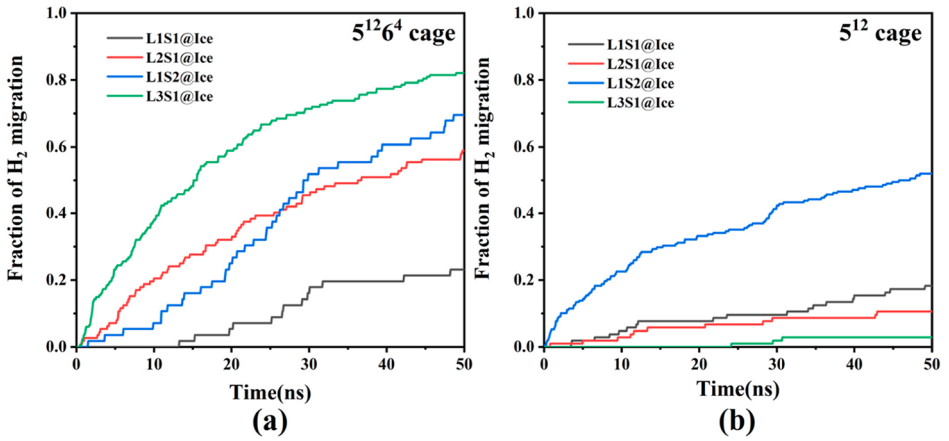


Figure 12. Fraction of hydrogen migrating out from (a) $5^{12}6^4$ cages; (b) 5^{12} cages.

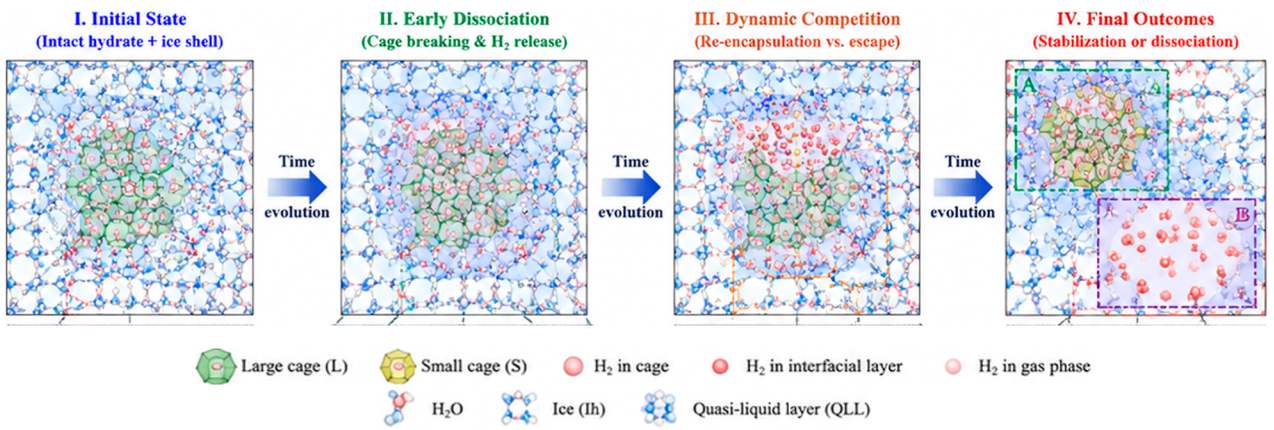


Figure 13. Mechanism of stabilization of hydrogen hydrate by ice shell.

molecules are more easily stabilized within the hydrate cages, which leads to expansion of the lattice parameters.[40,41] Conversely, the expansion of the lattice parameters further increased the additional pressure exerted by the ice on the hydrate. So, the ice phase gradually reacted with inward-diffusing H_2 to form new hydrate cages. This continuous ice-to-hydrate conversion consumed the outer ice shell layer by layer, thinning the ice crust until it lost its complete shielding structure and finally collapsed (equivalent to the macroscopic phenomenon of ice shell "melting"). By contrast, low-occupancy L1S1 system had weak hydrogen intercage migration. Few hydrogen molecules diffuse into the ice layer, so ice-to-hydrate phase transition barely occurred; the ice shell remained intact and even slightly thickens over simulation time without melting or collapse.

On the basis of the results of this study, a mechanism for the stabilization of hydrogen hydrates with an ice Ih shell was proposed (Figure 13). For the hydrogen hydrates with an ice Ih shell system, the ice shell provided an effective barrier to hydrogen diffusion and simultaneously exerted additional pressure on the hydrogen hydrates, thereby stabilizing the hydrate structure even under superheated conditions. During hydrate dissociation, a hydrogen-rich interfacial region (quasi-liquid layer) was formed. In this region, water molecules exhibited partially disordered hydrogen-bonding networks, which created transient cavities structurally similar to hydrate cages. Ice Ih possessed a highly ordered, dense hydrogen-bonded hexagonal network. Free hydrogen molecules encounter enormous steric resistance when they attempt to pass through intact bulk ice. As a result, the escaped hydrogen molecules induced a structural transformation between hydrate and ice within this confined space. During the process, structural transformations between the ice and hydrate phases occurred, which were also related to the additional pressure. The process was strongly correlated with the hydrogen cage occupancy in the hydrate. For low-cage occupancy systems (the L1S1@Ice system), the additional pressure exerted by the ice shell was insufficient to stabilize the hydrogen hydrate structure, resulting in the collapse of the hydrate structure and the transformation of water molecules into the ice structure. Due to the strong hydrogen-blocking effect of the ice shell, hydrogen molecules can migrate back into the hydrate cages, causing lattice expansion and an increase in the additional pressure until a stable structural equilibrium was achieved. The protective effect of the ice shell depends strongly on the hydrogen cage occupancy of the hydrate. When the structural transformation between ice and hydrogen hydrate reaches equilibrium, the critical hydrogen occupancy in the $5^{12}6^4$ cages was approximately 1.5 (see Supporting Information Figure S3). For high-cage occupancy systems (L2S1@Ice, L1S2@Ice, and L3S1@Ice), hydrogen molecules would overcome the confinement of hydrate cages and migrate to the ice phase, leading to the transformation of a part of the ice shell into a hydrate structure. As a result, the ice shell gradually thinned until structural failure occurred. However, in the Extended-Ice system, hydrogen migration to the ice shell would lead to a gradual decrease in cage

https://doi.org/10.1021/acs.energyfuels.6c02515
Energy Fuels 2026, 40, 17616−17626

Downloaded from pubs.acs.org/enfuem/article-pdf/40/32/17616/6335445/acs.energyfuels.6c02515.pdf by SOUTH CHINA UNIV OF TECHNOLOGY user on 02 November 2026

occupancy. When the system reached the critical cage occupancy, the outermost ice shell still existed, allowing the ice shell to effectively stabilize the hydrogen hydrate structure.

4. CONCLUSION

This study systematically investigated the stability of hydrogen hydrates with ice Ih shell systems with different initial cage occupancies at 260 K and 10 MPa by MD simulations. The dissociation behavior of hydrogen hydrates and the stabilization mechanism were revealed at the molecular level. The main conclusions are summarized as follows:

1 At 260 K and 10 MPa, a quasi-liquid film caused by hydrate dissociation increased the diffusion resistance for hydrogen molecules migrating from the hydrate phase to the gas phase. Different kinetic dissociation characteristics were observed with the hydrogen cage occupancy. However, all hydrogen hydrate systems eventually dissociated completely, indicating that hydrogen hydrates were thermodynamically unstable under the conditions.

2 The stability of hydrogen hydrates with an ice Ih shell was strongly dependent on the hydrogen cage occupancy. In the L1S1@Ice system, hydrogen hydrates remained stable and achieved superheated preservation. In the L2S1@Ice, L1S2@Ice, and L3S1@Ice systems, hydrate and ice structures disappeared after the simulation. Nevertheless, the presence of the ice shell significantly prolonged the hydrate dissociation time, thereby inhibiting the dissociation process.

3 The stabilization mechanism of hydrogen hydrates with ice shell was elucidated by potential energy, configuration, fraction of hydrogen migration, and hydrogen diffusion coefficient analysis. The structural transformation at the ice−hydrate interface was identified as the key mechanism controlling hydrate stability, which was highly correlated with the hydrogen cage occupancy. The optimal hydrogen occupancy of the $5^{12}6^4$ cages was approximately 1.5. When the occupancy was below the optimal value, hydrates at the interface transformed into ice. And hydrogen hydrates can be stably preserved as the shielding effect of the ice shell. When the occupancy was above the optimal value, hydrogen molecules migrating outward from the hydrate combined with ice to form hydrate structures, the ice shell would gradually thin and eventually collapse, making stable preservation of hydrogen hydrates impossible.

This study elucidates the molecular-level stabilization mechanism of the ice shell on hydrogen hydrates and clarifies the regulation effects of cage occupancy on hydrogen hydrates stability. These findings provide theoretical guidance for the design of highly stable hydrate-based hydrogen storage and transportation systems.

■ ASSOCIATED CONTENT

Supporting Information

The Supporting Information is available free of charge at https://pubs.acs.org/doi/10.1021/acs.energyfuels.6c02515.

Methodology: data analysis of potential energy, configuration, number of water molecules, fraction of hydrogen migration, density distribution, diffusion coefficient, and number of hydrate cages; Supplementary Figure 1: the initial configuration of hydrogen hydrate system; Supplementary Figure 2: snapshots of hydrogen hydrate dissociation and time evolution of cages with hydrogen molecules of the L1S2 system; and Supplementary Figure 3: the number of cages in the L1S1@Ice system (PDF)

■ AUTHOR INFORMATION

Corresponding Author

Yanhong Wang − *School of Chemistry and Chemical Engineering, South China University of Technology, Guangzhou 510640, China; Key Laboratory of Heat and Mass Transfer and Low-Carbon Conversion, Ministry of Education, Guangzhou 510640, China;* orcid.org/0000-0002-0059-8159; Email: wyh@scut.edu.cn

Authors

Siyuan Chen − *School of Chemistry and Chemical Engineering, South China University of Technology, Guangzhou 510640, China;* orcid.org/0000-0001-9839-6493

Yang Du − *School of Chemistry and Chemical Engineering, South China University of Technology, Guangzhou 510640, China*

Xin Lv − *Ningbo Institute of Dalian University of Technology, Ningbo 315016, China;* orcid.org/0000-0003-3683-6419

Shuanshi Fan − *School of Chemistry and Chemical Engineering, South China University of Technology, Guangzhou 510640, China; Key Laboratory of Heat and Mass Transfer and Low-Carbon Conversion, Ministry of Education, Guangzhou 510640, China;* orcid.org/0000-0002-2227-7620

Xuemei Lang − *School of Chemistry and Chemical Engineering, South China University of Technology, Guangzhou 510640, China; Key Laboratory of Fuel Cell Technology of Guangdong Province, Guangzhou 510640, China;* orcid.org/0000-0002-3189-7290

Gang Li − *School of Chemistry and Chemical Engineering, South China University of Technology, Guangzhou 510640, China;* orcid.org/0000-0001-5197-3425

Complete contact information is available at: https://pubs.acs.org/10.1021/acs.energyfuels.6c02515

Author Contributions

Siyuan Chen: conceptualization, investigation, formal analysis, writing—original draft; Yang Du: methodology, visualization; Yanhong Wang: project administration, conceptualization, writing—review and editing, Supervision; Xin Lv: writing—review and editing, formal analysis; Shuanshi Fan: project administration, supervision; Xuemei Lang: data curation; Gang Li: validation.

Notes

The authors declare no competing financial interest.

■ ACKNOWLEDGMENTS

This work was supported by the National Natural Science Foundation of China (52576205).

■ REFERENCES

(1) Israr, A.; Saadat, M.; Israr, A.; Rehman, A.; Junaid, M. Green hydrogen energy, current trends, challenges and future developments. *Sustain. Energy Technol. Assessments* **2026**, *86*, 104886.

(2) Etezadi, R.; Shivaramakrishnan, S.; Tsotsis, T. T.; et al. Hydrogen storage methods, materials, and challenges: scientific exploration. *Ind. Eng. Chem. Res.* **2026**, *65* (3), 1403−1423.

Downloaded from pubs.acs.org/enfuem/article-pdf/40/32/17616/6335445/acs.energyfuels.6c02515.pdf by SOUTH CHINA UNIV OF TECHNOLOGY user on 02 November 2026

(3) Profio, P.; Arca, S.; Rossi, F.; Filipponi, M. Comparison of hydrogen hydrates with existing hydrogen storage technologies: Energetic and economic evaluations. *Int. J. Hydrogen Energy* **2009**, *34*, 9173−9180.
(4) Sloan, E. D.; Carolyn, K. *Clathrate Hydrates of Natural Gases*, thrid ed. ed., 2007; . M.
(5) Mao, W. L.; Mao, H. k.; Goncharov, A. F.; Struzhkin, V. V.; Guo, Q.; Hu, J.; Shu, J.; Hemley, R. J.; Somayazulu, M.; Zhao, Y. Hydrogen clusters in clathrate hydrate [J]. *Science* **2002**, *297* (5590), 2247−2249.
(6) Mao, W.; Mao, H. Hydrogen storage in molecular compounds [J]. *Proc. Natl. Acad. Sci. U. S. A.* **2004**, *101* (3), 708−710.
(7) Stern, L. A.; Circone, S.; Kirby, S. H.; et al. Anomalous preservation of pure methane hydrate at 1 atm. *J. Phys. Chem. B* **2001**, *105* (9), 1756−1762.
(8) Takeya, S.; Ripmeester, J. A. Dissociation behavior of clathrate hydrates to ice and dependence on guest molecules. *Angew. Chem., Int. Ed.* **2008**, *47* (7), 1276−1279.
(9) Takeya, S.; Yoneyama, A.; Ueda, K.; et al. Nondestructive imaging of anomalously preserved methane clathrate hydrate by phase contrast X-ray imaging[J]. *J. Phys. Chem. C* **2011**, *115* (32), 16193−16199.
(10) Melnikov, V. P.; Nesterov, A. N.; Reshetnikov, A. M.; et al. Evidence of liquid water formation during methane hydrates dissociation below the ice point[J]. *Chem. Eng. Sci.* **2009**, *64* (6), 1160−1166.
(11) Lang, X. M.; Wang, Y. H.; Fan, S. S.; et al. Similar self-preservation and decomposition kinetics of tetrahydrofuran-hydrogen hydrate particles. *Int. J. Hydrogen Energy* **2022**, *47* (13), 8457−8466.
(12) Sharifi, H.; Yoneyama, A.; Takeya, S.; et al. Superheating clathrate hydrates for anomalous preservation[J]. *J. Phys. Chem. C* **2018**, *122* (30), 17019−17023.
(13) Takeya, S.; Muromachi, S.; Yoneyama, A.; et al. Superheating of structure I gas hydrates within the structure II cyclopentane hydrate shell[J]. *J. Phys. Chem. Lett.* **2022**, *13* (9), 2130−2136.
(14) Wang, S.; Xu, J.; Fan, S.; et al. Atmospheric preservation of CH4 hydrate above ice point: a potential application for high-density natural gas storage under moderate conditions[J]. *Fuel* **2021**, *293*, 120482.
(15) Zhong, H.; Li, L.; Ma, R.; Zhong, J.; Yan, Y.; Li, S.; Zhang, J.; Liu, J. Two-dimensional hydrogen hydrates: structure and stability. *Phys. Chem. Chem. Phys.* **2020**, *22*, 5774−5784.
(16) Krishnan, Y.; Ghaani, M. R.; English, N. J. Hydrogen and Deuterium Molecular Escape from Clathrate Hydrates: "Leaky" Microsecond-Molecular-Dynamics Predictions. *J. Phys. Chem. C* **2021**, *125*, 8430−8439.
(17) English, N. J.; Burnham, C. J. Intra-Cage Structure, Vibrations and Tetrahedral-Site Hopping of H_2 and D_2 in Doubly-Occupied $5^{12}6^4$ Cages in sII Clathrate Hydrates from Path-Integral and Classical Molecular Dynamics. *Appl. Sci.* **2021**, *11*, 54.
(18) Gorman, P. D.; English, N. J.; Macelroy, J. M. D. Dynamical cage behaviour and hydrogen migration in hydrogen and hydrogen-tetrahydrofuran clathrate hydrates. *J. Chem. Phys.* **2012**, *136*, 044506.
(19) Krishnan, Y.; Ghaani, M. R.; Desmedt, A.; English, N. J. Hydrogen Inter-Cage Hopping and Cage Occupancies inside Hydrogen Hydrate: Molecular-Dynamics Analysis. *Appl. Sci.* **2021**, *11*, 282.
(20) Burnham, C. J.; Futera, Z.; English, N. J. Quantum and classical inter-cage hopping of hydrogen molecules in clathrate hydrate: temperature and cage-occupation effects. *Phys. Chem. Chem. Phys.* **2017**, *19*, 717−728.
(21) Abascal, J. L. F.; Sanz, E.; Fernandez, R. G.; et al. A potential model for the study of ices and amorphous water: TIP4P/Ice[J]. *J. Phys.−Chem.* **2005**, *122* (23), 234511.
(22) Alavi, S.; Ripmeester, J. A.; Klug, D. D. Molecular-dynamics study of structure II hydrogen clathrates[J]. *J. Phys.−Chem.* **2005**, *123* (2), 24507.
(23) Kong, C. L. Combining rules for intermolecular potential parameters. II. rules for the Lennard-Jones (12−6) potential and the morse potential[J]. *J. Chem. Phys.* **1973**, *59* (5), 2464−2467.
(24) Luis, D. P.; Romero-Ramirez, I. E.; Gonzalez-Calderon, A.; López-Lemus, J. The coexistence temperature of hydrogen clathrates: A molecular dynamics study[J]. *J. Chem. Phys.* **2018**, *148* (11), 114503.
(25) Garcia Fernandez, R.; Abascal, J. L.; Vega, C. The melting point of ice Ih for common water models calculated from direct coexistence of the solid-liquid interface[J]. *J. Chem. Phys.* **2006**, *124* (14), 144506.
(26) Frankcombe, T. J.; Kroes, G. J. Molecular dynamics simulations of Type-sII hydrogen clathrate hydrate close to equilibrium conditions. *J. Phys. Chem. C* **2007**, *111* (35), 13044−13052.
(27) Takeuchi, F.; Hiratsuka, M.; Ohmura, R.; Alavi, S.; Sum, A. K.; Yasuoka, K. Water proton configurations in structures I, II, and H clathrate hydrate unit cells[J]. *J. Chem. Phys.* **2013**, *138* (12), 124504.
(28) Hayward, J. A.; Reimers, J. R. Unit cells for the simulation of hexagonal ice[J]. *J. Chem. Phys.* **1997**, *106* (4), 1518−1529.
(29) Nguyen, A. H.; Koc, M. A.; Shepherd, T. D.; et al. Structure of the ice−clathrate interface[J]. *J. Phys. Chem. C* **2015**, *119* (8), 4104−4117.
(30) Abraham, M. J.; Murtola, T.; Schulz, R.; et al. GROMACS: high performance molecular simulations through multi-level parallelism from laptops to supercomputers[J]. *SoftwareX* **2015**, *1−2*, 19−25.
(31) Nosé, S. A molecular dynamics method for simulations in the canonical ensemble[J]. *Mol. Phys.* **1984**, *52* (2), 255−268.
(32) Parrinello, M.; Rahman, A. Polymorphic transitions in single crystals: a new molecular dynamics method[J]. *J. Appl. Phys.* **1981**, *52* (12), 7182−7190.
(33) Essmann, U.; Perera, L.; Berkowitz, M. L.; et al. A smooth particle mesh ewald method[J]. *J. Chem. Phys.* **1995**, *103* (19), 8577−8593.
(34) Lokshin, K. A.; Zhao, Y. S. Fast synthesis method and phase diagram of hydrogen clathrate hydrate[J]. *Appl. Phys. Lett.* **2006**, *88* (13), 131909.
(35) Ding, L.; Geng, C.; Zhao, Y.; et al. Molecular dynamics simulation for surface melting and self-preservation effect of methane hydrate[J]. *Sci. China, Ser. B:Chem.* **2008**, *51* (7), 651−660.
(36) Li, K. H.; Chen, B. B.; Song, Y. C.; et al. Molecular dynamics simulation of the effects of different thermodynamic parameters on methane hydrate dissociation: An analysis of temperature, pressure and gas concentrations[J]. *Fluid Phase Equilib.* **2020**, *516*, 112606.
(37) Hasegawa, T.; Brumby, P. E.; Yasuoka, K.; Sum, A. K. Mechanism for H_2 diffusion in sII hydrates by molecular dynamics simulations[J]. *J. Chem. Phys.* **2020**, *153*, 054706.
(38) Nguyen, A. H.; Molinero, V. Identification of clathrate hydrates, hexagonal ice, cubic ice, and liquid water in simulations: the CHILL+ algorithm[J]. *J. Phys. Chem. B* **2015**, *119* (29), 9369−9376.
(39) Belosudov, R. V.; Bozhko, Y. Y.; Zhdanov, R. K.; et al. Hydrogen hydrates: equation of state and self-preservation effect[J]. *Fluid Phase Equilib.* **2016**, *413*, 220−228.
(40) Chen, S. Y.; Wang, Y. H.; Fan, S. S.; et al. Intriguing phenomenon of hydrogen molecules occupancy in clathrate hydrate cages: Implications for hydrogen storage[J]. *Chemical Engineering Journal* **2024**, *499*, 156089.
(41) Chen, S. . y.; Li, X. Y.; Wang, Y. H.; et al. Efficient hydrogen storage in hydrate solid solution: Structural insights and performance-[J]. *Int. J. Hydrogen Energy* **2026**, *204*, 153331.

Downloaded from pubs.acs.org/enfuem/article-pdf/40/32/17616/6335445/acs.energyfuels.6c02515.pdf by SOUTH CHINA UNIV OF TECHNOLOGY user on 02 November 2026

https://doi.org/10.1021/acs.energyfuels.6c02515
Energy Fuels 2026, 40, 17616−17626